Díez, P., Parés; N. and Huerta, A., Recovering lower bounds of the error by postprocessing implicit residual a posteriori error estimates, *International Journal for Numerical Methods in Engineering*, Vol. 56, Issue 10, pp. 1465-1488, 2003

Recovering lower bounds of the error by postprocessing implicit residual *a posteriori* error estimates

Pedro Díez, Núria Parés and Antonio Huerta*,†

Departament de Matemàtica Aplicada III, ETSECCPB, Universidad Politécnica de Cataluña, Barcelona, Spain

SUMMARY

Classical residual type error estimators approximate the error flux around the elements and yield upper bounds of the exact (or reference) error. Lower bounds of the error are also needed in goal oriented adaptivity and for bounds on functional outputs. This work introduces a simple and cheap strategy to recover a lower bound estimate from standard upper bound estimates. This lower bound may also be used to assess the effectivity of the former estimate and to improve it.

KEY WORDS: implicit residual type error estimator; upper and lower bounds; quality assessment

1. INTRODUCTION

Implicit residual-type error estimators require to set proper boundary conditions for the local (usually element by element) error equations. If these boundary conditions are of Neumann type [1, 2] the obtained estimates are upper bounds of the error. The error estimators based on the error in the constitutive relation introduced by Ladevèze [3, 4] may also be classified in this group and also overestimate the error. The selection of the flux on the interelement edges may use either a trivial flux averaging [1] or a more sophisticated recovering technique yielding equilibrated residuals [2, 3]. The equilibrated residual strategies are expected to furnish more realistic boundary conditions for the local problems and, consequently, to yield better error estimates.

On the other hand, residual-type error estimators using Dirichlet boundary conditions in the local error equations [5, 6] yield lower bounds of the error. Basically, the lower bound property is induced by the continuity of the obtained estimate.

*Correspondence to: Antonio Huerta, Departament de Matemàtica Aplicada III, ETSECCPB, Universidad Politécnica de Cataluña, Campus Norte UPC, Módule C-2, Jordi Giruna 1, E-08034 Barcelona, Spain
†E-mail: antonio.huerta@upc.es

Contract/grant sponsor: Ministerio de Educación y Cultura; contract/grant number: TAP98-0421

The comparison of these two approaches suggest the idea of postprocessing residual-type error estimators yielding upper bound, enforcing continuity and obtaining a lower bound of the error with a small supplementary effort.

The idea of obtaining a couple of upper and lower bound estimates at the same time is also suggested by the goal oriented adaptive strategies [7, 8]. Indeed, in the context of symmetric (self-adjoint) problems, these strategies require both a lower and an upper bound of the error in the standard energy norm to assess the error in an output of interest. However, the approach introduced in Reference [8] allows also to obtain upper and lower bounds for functional outputs of non-symmetric problems.

The approach presented here is based on the postprocessing of the upper bound estimate e_{est}, which is discontinuous. The postprocessing introduces a correction e_{cor} such that the corrected error distribution, $e_{\text{cont}} := e_{\text{est}} + e_{\text{cor}}$, is continuous. Thus, the correction e_{cor} must compensate the discontinuities of e_{est}. Then, a lower bound is computed straightforward using e_{est} and e_{cor}.

The remainder of the paper is structured as follows. The model problem is stated in Section 2. Section 3 is devoted to introduce the local and global versions of error equation, and the reference error. In Section 4, the residual-type error estimators approximating the local flux are described. The upper bound property of this kind of estimators is easily proved. Attention is paid to the solvability problems of the pure diffusion case. Then, in Section 5, the estimate e_{est} yielding an upper bound is corrected to enforce its continuity and a lower bound is recovered. Also at this point, some additional effort must be done to deal with the pure diffusion case, where the original estimate is locally determined up to a constant. These local constants do not affect the norm of e_{est} but do condition e_{cor} and, consequently, in order to have an optimal correction, it is worthy to select them properly. Numerical examples demonstrating the good behaviour of the proposed strategy are shown in Section 6.

2. STATEMENT OF THE PROBLEM

2.1. Model problem

Let us consider the following linear Neumann boundary value problem in an open, bounded domain $\Omega \subset \mathbb{R}^2$

$$\left.\begin{aligned} -\nabla \cdot (a\nabla u) + bu = s \quad & \text{in } \Omega \\ a\nabla u \cdot n = g_N \quad & \text{on } \partial\Omega \end{aligned}\right\} \tag{1}$$

In order to simplify the presentation, the boundary conditions are assumed to be only of Neumann type. Accounting for Dirichlet or mixed boundary conditions does not introduce any additional conceptual difficulty. Moreover, in order to ensure ellipticity, it is assumed that

$$0 < \underline{a} \leqslant a(x) \leqslant \bar{a}$$

$$0 \leqslant \underline{b} \leqslant b(x) \leqslant \bar{b}$$

for some $\underline{a}$, $\bar{a}$, $\underline{b}$ and $\bar{b}$.

The weak form of this problem reads: find $u \in H^1(\Omega)$ such that

$$a(u,v) = \int_\Omega sv \,\mathrm{d}\Omega + \int_{\partial\Omega} g_N v \,\mathrm{d}\Gamma \quad \forall v \in H^1(\Omega) \tag{2}$$

where

$$a(u,v) := \int_\Omega (a\nabla u \cdot \nabla v + buv) \,\mathrm{d}\Omega$$

and $H^1(\Omega)$ stands for the standard Sobolev space.

The Galerkin finite element method provides an approximation u_h to u, lying in a finite-dimensional space $V_h \subset H^1(\Omega)$ and verifying

$$a(u_h,v) = \int_\Omega sv \,\mathrm{d}\Omega + \int_{\partial\Omega} g_N v \,\mathrm{d}\Gamma \quad \forall v \in V_h \tag{3}$$

The finite-dimensional space V_h is associated with a finite element mesh of characteristic size h. The degree of the complete polynomials used in the interpolation of V_h is denoted by p. The geometric support of the elements of this mesh are open subdomains denoted by $\Omega_k,\ k = 1,\ldots,\mathrm{n_{elem}}$. It is assumed that $\bar{\Omega} = \bigcup_k \bar{\Omega}_k$ (the mesh covers the whole domain) and $\Omega_k \cap \Omega_l = \emptyset$ for $k \neq l$ (different elements have in common, at most, part of their boundary). The derivation of *a priori* estimates requires further regularity conditions for the mesh. The precise assumptions on the meshes may be found in Reference [9, Section 1.3.3].

The goal of *a posteriori* error estimation is to assess the accuracy of the approximate solution u_h, that is, to evaluate and measure the error, $e := u - u_h$, or an approximation to it. The error is measured using some functional norm. One of the most popular options is the energy norm induced by $a(\cdot,\cdot)$:

$$\|e\| := [a(e,e)]^{1/2} \tag{4}$$

Local restrictions of the norm are needed to describe the spatial distribution of the error. In the following, the restriction of $a(\cdot,\cdot)$ to the element Ω_k $(k = 1,\ldots,\mathrm{n_{elem}})$ is denoted by $a_k(\cdot,\cdot)$. Thus, the restriction of $\|\cdot\|$ to $\Omega_k,\ \|\cdot\|_k$, is induced by $a_k(\cdot,\cdot)$. In order to describe the spatial distribution of the error, the value of $\|e\|_k$ in each element is estimated.

2.2. Error equations and reference error

The global equation for the error is recovered from Equation (2), replacing u by $u_h + e$:

$$a(e,v) = \int_\Omega sv \,\mathrm{d}\Omega + \int_{\partial\Omega} g_N v \,\mathrm{d}\Gamma - a(u_h,v) =: \mathbf{R}(v) \quad \forall v \in H^1(\Omega) \tag{5}$$

The r.h.s. term of Equation (5), $\mathbf{R}(v)$, is the weak residual associated with the approximate solution u_h.

The local counterpart of Equation (5) is derived integrating the weighted residual of the strong form, Equation (1), in Ω_k. It reads,

$$a_k(e,v) = \mathbf{R}_k(v) + \int_{\partial\Omega_k \cap \Omega} a\nabla u \cdot n v \,\mathrm{d}\Gamma \quad \forall v \in H^1(\Omega_k) \tag{6}$$

where $\mathbf{R}_k(v)$ is the restriction of $\mathbf{R}(v)$ to Ω_k:

$$\mathbf{R}_k(v) := \int_{\Omega_k} sv \, \mathrm{d}\Omega + \int_{\partial\Omega_k \cap \partial\Omega} g_N v \, \mathrm{d}\Gamma - a_k(u_h, v) \tag{7}$$

Note that the last term of the r.h.s. of Equation (6) accounts for the unknown flux on the interelement edges. In other words, the boundary conditions of the local problem are not known.

The error is estimated approximating the solution of the local error equation (6). The characterization of any residual-type error estimator requires to select both:

- the finite-dimensional space where the local error equation is solved (local *h*- or *p*-refinement) and
- the unknown boundary conditions for the local problems.

The first point is related with the concept of reference error. Residual *a posteriori* error estimation techniques are based on assessing and bounding the reference error and not the error itself. For all practical purposes, the exact value of the error, e, is replaced by a reference (or 'truth') error, e_{ref}, lying in a finite-dimensional space much refined with respect to the computational space V_h. Let us denote by V^{ref} this refined space. V^{ref} is generated either as a h or p-refinement of V_h. That is, denoting by $\tilde{h}$ and $\tilde{p}$ the characteristic element size and the degree of interpolation of the elements generating V^{ref}, either $\tilde{h} \ll h$ or $\tilde{p} \gg p$ holds.

Thus, the reference error, $e_{\mathrm{ref}} \in V^{\mathrm{ref}}$, verifies the discrete form of Equation (5), that is

$$a(e_{\mathrm{ref}}, v) = \mathbf{R}(v) \quad \forall v \in V^{\mathrm{ref}} \tag{8}$$

The direct computation of e_{ref} is computationally unaffordable because it requires to solve a system of equations with the number of degrees of freedom equal to the dimension of V^{ref}.

The fact of using a reference error (that is, replacing the continuous space $H^1(\Omega)$ by the refined space V^{ref}, and the exact error e by the reference error e_{ref}) does not introduce a significant loss of accuracy in the error estimation procedure. Consequently, the quality of a residual-type error estimation procedure depends essentially on the approximation of the local boundary conditions.

3. STANDARD RESIDUAL-TYPE ERROR ESTIMATES

Standard residual-type error estimators [1–3] solve the local error equation (6) using approximated Neumann boundary conditions. The values of the flux $a\nabla u \cdot n|_{\partial\Omega_k \cap \Omega}$, see Equation (6), are determined or approximated along the boundary of each element Ω_k. This section is devoted to briefly describe this kind of estimators and to recall the proof of their upper bound property.

3.1. Approximation of fluxes

The approximation of the flux is based on smoothing the approximate flux $a\nabla u_h \cdot n$, which is discontinuous. The basic idea due to Bank and Weiser [1] is to average the approximate flux on every interelement edge. Let Γ_m, for $m = 1, \ldots, \mathrm{n_{int}}$, be the interelement edges of the mesh.

That is, for every $m \in \{1, \ldots, \mathrm{n_{int}}\}$ they exist $k, l \in \{1, \ldots, \mathrm{n_{elem}}\}$, $k \neq l$, such that $\Gamma_m = \overline{\Omega_k} \cap \overline{\Omega_l}$. Then

$$a\nabla u|_{\Gamma_m} \simeq [a\nabla u_h]_A := \tfrac{1}{2}(a\nabla u_h|_{\partial\Omega_l} + a\nabla u_h|_{\partial\Omega_k}) \quad \text{for } m = 1, \ldots, \mathrm{n_{int}} \tag{9}$$

where $[\cdot]_A$ stands for the average on Γ_m. The approximation given in Equation (9) is used in Equation (6).

More sophisticated flux averaging procedures are used by other authors [2, 3] in order to obtain equilibrated local problems. They improve the efficiency of the estimator. Here, the simplest averaging is used for illustration purposes. In fact, the following developments are also valid for these approaches: it suffices to use a more complicated definition for the average $[a\nabla u_h]_A$.

3.2. Discrete local residual equation

Thus, the error estimate e_{est} is computed locally by solving the following problem: find $e_{\mathrm{est}} \in V_k^{\mathrm{ref}}$ such that

$$a_k(e_{\mathrm{est}}, v) = \mathbf{R}_k(v) + \int_{\partial\Omega_k \cap \Omega} [a\nabla u_h]_A \cdot nv \, \mathrm{d}\Gamma \qquad \forall v \in V_k^{\mathrm{ref}} \tag{10}$$

where V_k^{ref} is the restriction of V^{ref} to Ω_k, that is

$$V_k^{\mathrm{ref}} := \{v \in H^1(\Omega_k) / \exists \tilde{v} \in V^{\mathrm{ref}}, \ v = \tilde{v}|_{\Omega_k}\} \tag{11}$$

Equation (10) is the discrete version of Equation (6) using the approximation given by Equation (9).

Note that the sum of the spaces V_k^{ref} is not equal to V^{ref}. In fact, $V_{\mathrm{brok}}^{\mathrm{ref}} := \bigoplus_k V_k^{\mathrm{ref}}$ is a space of 'broken' functions. In order to recover V^{ref} it is necessary to restrict the space forcing the continuity: $V^{\mathrm{ref}} = V_{\mathrm{brok}}^{\mathrm{ref}} \cap \mathscr{C}^0$.

A global equation for the error estimate e_{est} is found summing up Equation (10) for all k $(k = 1, \ldots, \mathrm{n_{elem}})$,

$$a(e_{\mathrm{est}}, v) = \mathbf{R}(v) + \sum_{m=1}^{\mathrm{n_{int}}} \int_{\Gamma_m} [a\nabla u_h]_A \cdot [vn]_J \, \mathrm{d}\Gamma \quad \forall v \in V_{\mathrm{brok}}^{\mathrm{ref}} \tag{12}$$

where $[vn]_J$ stands for the jump of vn across $\Gamma_m = \overline{\Omega_k} \cap \overline{\Omega_l}$, that is,

$$[vn]_J := (v|_{\Omega_k})n_k + (v|_{\Omega_l})n_l \tag{13}$$

being $n_k = -n_l$ the corresponding outward normal unit vectors. The recovered flux, see Section 3.1, is said to be consistent if the approximation of the flux is continuous, i.e. if the approximation of $a\nabla u|_{\Gamma_m}$ is the same viewed from Ω_k and from Ω_l. In order to derive Equation (12) it is necessary that the recovered fluxes are consistent.

Furthermore, if the test functions are continuous, i.e. if v is in $V^{\mathrm{ref}} \subset V_{\mathrm{brok}}^{\mathrm{ref}}$, then $[vn]_J = 0$ and from Equation (12) one gets

$$a(e_{\mathrm{est}}, v) = \mathbf{R}(v) \quad \forall v \in V^{\mathrm{ref}}, \text{ where still } e_{\mathrm{est}} \in V_{\mathrm{brok}}^{\mathrm{ref}} \tag{14}$$

In other words, if the consistency condition is satisfied, the interelement edges are not a source of flux in the global error equation (for v continuous). In the following, some properties of the estimate e_{est} are derived replacing v in Equation (14) by particular functions in V^{ref}.

Remark 1
In Equation (12), the definition of $a(\cdot,\cdot)$ must be generalized to accept 'broken' functions in the arguments. Thus, for $v, w \in V^{\text{ref}}_{\text{brok}}$,

$$a(w,v) := \sum_{k=1}^{n_{\text{elem}}} a_k(w,v) \tag{15}$$

Of course, this generalized definition coincides with the standard one when the arguments are in $H^1(\Omega)$.

3.3. Upper bound property

The consistency condition implies that the error estimates computed using Equation (10) are upper bounds of the reference error. Although this is a well-known property of this kind of estimators, the corresponding theorem is revisited and proved here because it is important in the following.

Theorem 1
The error estimate e_{est} computed solving Equation (10) yields an upper bound of the error, that is

$$\varepsilon_{\text{upp}} := \|e_{\text{est}}\|^2 \geqslant \|e_{\text{ref}}\|^2 \tag{16}$$

Proof
Taking $v = e_{\text{ref}}$ in Equations (14) and (8) it follows that

$$a(e_{\text{est}}, e_{\text{ref}}) = a(e_{\text{ref}}, e_{\text{ref}}) \tag{17}$$

Then, the proof is completed by the following algebraic manipulation.

$$\begin{aligned} 0 \leqslant a(e_{\text{ref}} - e_{\text{est}}, e_{\text{ref}} - e_{\text{est}}) &= a(e_{\text{ref}}, e_{\text{ref}}) + a(e_{\text{est}}, e_{\text{est}}) - 2\overbrace{a(e_{\text{est}}, e_{\text{ref}})}^{=a(e_{\text{ref}}, e_{\text{ref}})} \\ &= a(e_{\text{est}}, e_{\text{est}}) - a(e_{\text{ref}}, e_{\text{ref}}) \end{aligned}$$

□

Remark 2
It is worth noting that the upper bound ε_{upp} is defined in Equation (16) as the squared norm of the error estimate. This is because the use of squared norms simplifies the presentation. Thus, in the following, the estimates of the squared error norms, approximations of $\|e_{\text{ref}}\|^2$, are denoted by $\varepsilon_\star$.

Remark 3
In the general case, e_{est} is not continuous (it is in $V^{\text{ref}}_{\text{brok}}$ but not in V^{ref}). Thus, in general, it is not possible to take $v = e_{\text{est}}$ in Equation (14). However, if a particular choice of the boundary conditions of the local problems leads to a continuous estimate e_{est}, then it can be

easily shown that $a(e_{\text{est}}, e_{\text{est}}) \leqslant a(e_{\text{ref}}, e_{\text{ref}})$ and, consequently, $a(e_{\text{est}}, e_{\text{est}}) = a(e_{\text{ref}}, e_{\text{ref}})$. That is, the choice of the Neumann boundary conditions giving a continuous estimate is optimal.

3.4. Solvability problems when $b = 0$

If the reaction term vanishes in Equation (1) ($b = 0$), the solvability of the local Neumann problem, Equation (10), requires proper data ensuring equilibrium. It is well known that if the source term s (body load) is not equilibrated by the prescribed boundary flux, the Neumann problem does not have any solution. Locally (in element Ω_k), the equilibrium condition reads

$$\int_{\Omega_k} s \, \mathrm{d}\Omega + \int_{\partial\Omega_k \cap \partial\Omega} g_N \, \mathrm{d}\Gamma + \int_{\partial\Omega_k \cap \Omega} [a\nabla u_h]_A \cdot n \, \mathrm{d}\Gamma = 0 \tag{18}$$

The simple averaging described in Equation (9) does not enforce the equilibrium condition.

Two different strategies may be used in order to ensure the solvability of the local problems. A first option is to use approximation of fluxes yielding equilibrated local problems.

The second strategy is to restrict the set of admissible functions in the local problem eliminating from the local interpolation space the kernel of the l.h.s. of Equation (10). In fact, the second and third estimators introduced by Bank and Weiser in Reference [1] use this strategy. These estimators are used in the numerical examples and are they denoted by e_2 and e_3, respectively.

Remark 4

The description of these estimators requires to introduce the hierarchical decomposition of V^{ref}, $V^{\text{ref}} = V_h \oplus V^{\text{com}}$, where V^{com} is the hierarchical complement of V_h in V^{ref}. The space V^{com} contains the functions v of V^{ref} such that the degrees of freedom (nodal values) of v corresponding to V_h are null. Typically, for p-refinement, the functions of V^{com} are of the bubble type. Then, for all $v \in V^{\text{ref}}$, $\exists! v_h \in V_h$ and $\exists! v_{\text{com}} \in V^{\text{com}}$ such that $v = v_h + v_{\text{com}}$. Thus, the nodal projection from V^{ref} to V_h, $\mathscr{I} : V^{\text{ref}} \to V_h$ is defined such that $\mathscr{I}(v) = v_h$.

The second estimator, e_2 is then computed as the solution of the following local problem:

$$a_k(e_2, v) = \mathbf{R}_k(v - \mathscr{I}(v)) + \int_{\partial\Omega_k \cap \Omega} [a\nabla u_h]_A \cdot n(v - \mathscr{I}(v)) \, \mathrm{d}\Gamma \quad \forall v \in V_k^{\text{ref}} \tag{19}$$

where the restriction of e_2 to Ω_k is in V_k^{ref} and, therefore, the global e_2 is in $V_{\text{brok}}^{\text{ref}}$.

The third estimator, e_3, is locally computed as the solution of

$$a_k(e_3, v) = \mathbf{R}_k(v) + \int_{\partial\Omega_k \cap \Omega} [a\nabla u_h]_A \cdot nv \, \mathrm{d}\Gamma \quad \forall v \in V_k^{\text{com}} \tag{20}$$

where the local restriction of V^{com}, V_k^{com}, must be understood in the same sense as in Equation (11).

It is worth noting that e_2 is an upper bound for the reference error but e_3 is not. Indeed, summing up the local Equation (19) on k one gets a global equation for e_2 where v ranges on $V_{\text{brok}}^{\text{ref}}$ and the same rational given for e_{est}, see Theorem 1, can be followed to deduce that $\|e_2\| \geqslant \|e_{\text{ref}}\|$. On the contrary, in the global equation corresponding to Equation (20), v ranges on $V_{\text{brok}}^{\text{com}}$. The upper bound property cannot be deduced in this case because $V^{\text{ref}} \not\subset V_{\text{brok}}^{\text{com}}$. However, in the asymptotic range, that is for h small enough, numerical evidence shows that e_3 behaves also as an upper bound.

4. CORRECTION AND LOWER BOUND RECOVERING

In the previous section, see Remark 3, it has been noted that the overestimation of the error is associated with the continuity defaults of the estimate e_{est}. In fact, it has been observed that if the flux splitting is such that e_{est} is continuous, then the estimate e_{est} is optimal. Thus, the idea developed in this section is to introduce a correction of the error estimate in order to enforce its continuity. This correction allows to deduce a lower bound of the reference (and exact) error and, hence, to assess the effectivity of the original error estimate.

4.1. Correction and lower bound

Babuška and co-workers originally proposed to obtain a lower bound ε_{low} from a continuous corrected estimate [10, 11]. Here, the evaluation of the lower bound is improved by defining a scalar parametric family $\varepsilon_{\text{low}}(\lambda)$. Moreover, it is proved in this section that an optimal value of λ, λ_{opt} exists and that it can be easily evaluated. Note that the optimal estimate, $\varepsilon_{\text{low}}(\lambda_{\text{opt}})$ corresponds to the expression proposed in Reference [12], where the optimality of this choice is not mentioned.

Recall that $e_{\text{est}} \in V^{\text{ref}}_{\text{brok}}$, that is e_{est} is, in general, not continuous. Let $e_{\text{cor}} \in V^{\text{ref}}_{\text{brok}}$ be a correction of e_{est} such that

$$e_{\text{cont}} := e_{\text{est}} + e_{\text{cor}} \in V^{\text{ref}} \tag{21}$$

that is, such that the corrected error e_{cont} is continuous.

Given a corrected estimate e_{cont}, a parametric family of lower bound estimates is found.

Theorem 2

Let e_{est} be an error estimate verifying the hypothesis of Theorem 1 and, therefore, being an upper bound of the reference error. Let e_{cont} be a corrected estimate as described in Equation (21). Then, for any scalar $\lambda \in \mathbb{R}$, the expression

$$\varepsilon_{\text{low}}(\lambda) := 2\lambda a(e_{\text{est}}, e_{\text{cont}}) - \lambda^2 \|e_{\text{cont}}\|^2 \tag{22}$$

is a lower bound of the reference error norm, that is,

$$\varepsilon_{\text{low}}(\lambda) \leqslant \|e_{\text{ref}}\|^2 \tag{23}$$

Proof

Since e_{cont} is continuous, it is possible to replace v by e_{cont} in Equations (14) and (8). That is,

$$a(e_{\text{est}}, e_{\text{cont}}) = a(e_{\text{ref}}, e_{\text{cont}}) \tag{24}$$

Then, using Equation (24), inequality (23) is proved considering the following algebraic manipulation:

$$\begin{aligned} 0 \leqslant a(e_{\text{ref}} - \lambda e_{\text{cont}}, e_{\text{ref}} - \lambda e_{\text{cont}}) &= a(e_{\text{ref}}, e_{\text{ref}}) + \lambda^2 a(e_{\text{cont}}, e_{\text{cont}}) - 2\lambda a(e_{\text{ref}}, e_{\text{cont}}) \\ &= \|e_{\text{ref}}\|^2 + \lambda^2 \|e_{\text{cont}}\|^2 - 2\lambda a(e_{\text{est}}, e_{\text{cont}}) \\ &= \|e_{\text{ref}}\|^2 - \varepsilon_{\text{low}}(\lambda) \end{aligned}$$

□

Thus, once the corrected estimate e_{cont} is obtained, a lower bound of the error is recovered computing $\varepsilon_{\text{low}}(\lambda)$, for any value of λ. The natural choice, $\lambda = 1$, see References [10, 11, 13, 15], results in

$$\varepsilon_{\text{low}}(1) = 2a(e_{\text{est}}, e_{\text{cont}}) - \|e_{\text{cont}}\|^2 = \|e_{\text{est}}\|^2 - \|e_{\text{cor}}\|^2 \tag{25}$$

which in practice only requires the extra computation of $\|e_{\text{cor}}\|$.

However, the optimal choice for λ is the value that maximizes the lower bound $\varepsilon_{\text{low}}(\lambda)$. It is obvious from Equation (22) that this optimal value is

$$\lambda_{\text{opt}} = \frac{a(e_{\text{est}}, e_{\text{cont}})}{\|e_{\text{cont}}\|^2} \tag{26}$$

Consequently, given an upper bound estimate e_{est}, the optimal lower bound associated with a corrected estimate e_{cont} is

$$\varepsilon_{\text{low}}^{\text{opt}} := \varepsilon_{\text{low}}(\lambda_{\text{opt}}) = \frac{a(e_{\text{est}}, e_{\text{cont}})^2}{\|e_{\text{cont}}\|^2} \tag{27}$$

This is, in fact, the expression adopted in Reference [12].

Remark 5

Both $\varepsilon_{\text{low}}^{\text{opt}}$ and $\varepsilon_{\text{low}}(1)$ are exact if the recovering technique to obtain the corrected estimate e_{cont} is optimal. Indeed, if the corrected estimate coincides with the reference error, that is $e_{\text{cont}} = e_{\text{ref}}$, then

$$\varepsilon_{\text{low}}^{\text{opt}} = \varepsilon_{\text{low}}(1) = \|e_{\text{ref}}\|^2$$

Thus, both the lower bounds given by Equations (25) and (27) are sharp provided that the determination of the corrected estimate e_{cont} is accurate. In fact, the strategy used to obtain e_{cont} is oriented to enforce $e_{\text{cont}} \approx e_{\text{ref}}$.

Obviously, given e_{cont}, the estimate $\varepsilon_{\text{low}}^{\text{opt}}$ is sharper than $\varepsilon_{\text{low}}(1)$. Consequently, once e_{cont} is determined, $\varepsilon_{\text{low}}^{\text{opt}}$ is used to evaluate the lower bound. Nevertheless, in order to set a criterion for the determination of e_{cont}, the expression of $\varepsilon_{\text{low}}(1)$, Equation (25), is preferred to the expression of $\varepsilon_{\text{low}}^{\text{opt}}$, Equation (27). This is detailed in the next section.

4.2. Determination of the corrected estimate e_{cont}

This section describes the smoothing process that builds up the corrected estimate e_{cont}. The degrees of freedom of the original estimate, e_{est}, affecting the continuity (associated with edges and corners) are simply averaged. This part of the smoothing process is standard [10, 11]. Here, the remaining degrees of freedom affecting the interior of the elements (bubble functions inside the elements) are set using an objective optimality criterion. The presentation is based in the formulation of the parametric family of scalar lower bounds, $\varepsilon_{\text{low}}(\lambda)$ introduced in Section 4.1.

The correction e_{cor} and, consequently, the corrected estimate e_{cont} and the corresponding lower bound $\varepsilon_{\text{low}}^{\text{opt}}$ are not unique. Any function $e_{\text{cont}} \in V^{\text{ref}}$ produces a lower bound $\varepsilon_{\text{low}}^{\text{opt}}$. However, as noted in Remark 5, in order to obtain a sharp lower bound e_{cont} must be selected in order to fairly approximate e_{ref}. Assuming that e_{est} is a proper approximation of e_{ref} but

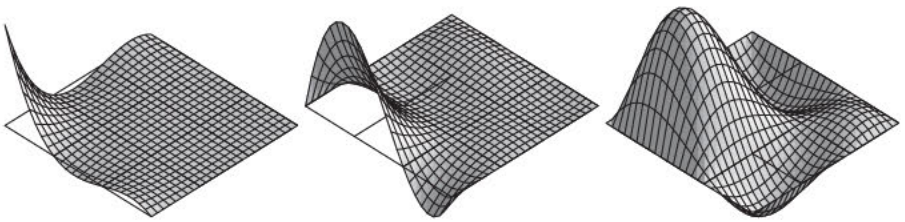

Figure 1. Classification and denomination of the interpolation functions in $V^{\text{ref}}_{\text{brok}}$. The functions affecting the boundaries, both associated with corners (left) and edges (centre) are responsible of the continuity. The interior bubble functions (right) do not affect the continuity and they are set in order to obtain the sharper lower bound ε_{low}.

in a broken space, a natural choice is to take the average of the estimated error along the interelement edges.

In order to formalize this averaging, the following decomposition of the local reference interpolation space V^{ref}_k is considered:

$$V^{\text{ref}}_k = V^{\text{corner}}_k \oplus V^{\text{edge}}_k \oplus V^{\text{bubble}}_k \tag{28}$$

where V^{bubble}_k is the subspace containing the bubble functions (vanishing on $\partial\Omega_k$), V^{edge}_k contains the functions having non-zero values in the boundary and vanishing in the corner nodes of element Ω_k and V^{corner}_k accounts for the degrees of freedom associated with the corner nodes, see Figure 1 for an illustration. This local decomposition induces the definition of the following global spaces:

$$\begin{aligned} V^{\text{corner}}_{\text{brok}} &:= \bigoplus_k V^{\text{corner}}_k \qquad V^{\text{corner}} := V^{\text{corner}}_{\text{brok}} \cap V^{\text{ref}} \\ V^{\text{edge}}_{\text{brok}} &:= \bigoplus_k V^{\text{edge}}_k \qquad V^{\text{edge}} := V^{\text{edge}}_{\text{brok}} \cap V^{\text{ref}} \\ V^{\text{bubble}} &:= \bigoplus_k V^{\text{bubble}}_k \end{aligned}$$

Note that V^{bubble} does not have a 'broken' version because the bubble functions do not introduce discontinuities along the edges. Thus, $V^{\text{ref}}_{\text{brok}}$ and V^{ref} are decomposed as

$$V^{\text{ref}}_{\text{brok}} = V^{\text{corner}}_{\text{brok}} \oplus V^{\text{edge}}_{\text{brok}} \oplus V^{\text{bubble}} \text{ and } V^{\text{ref}} = V^{\text{corner}} \oplus V^{\text{edge}} \oplus V^{\text{bubble}} \tag{29}$$

Consequently, the estimate e_{est} is uniquely represented by the following decomposition:

$$e_{\text{est}} = e^{\text{corner}}_{\text{est}} + e^{\text{edge}}_{\text{est}} + e^{\text{bubble}}_{\text{est}} \tag{30}$$

where $e^{\text{corner}}_{\text{est}} \in V^{\text{corner}}_{\text{brok}}$, $e^{\text{edge}}_{\text{est}} \in V^{\text{edge}}_{\text{brok}}$ and $e^{\text{bubble}}_{\text{est}} \in V^{\text{bubble}}$, and $e_{\text{cont}} \in V^{\text{ref}}$ is uniquely decomposed as

$$e_{\text{cont}} = e^{\text{corner}}_{\text{cont}} + e^{\text{edge}}_{\text{cont}} + e^{\text{bubble}}_{\text{cont}} \tag{31}$$

where $e^{\text{corner}}_{\text{cont}} \in V^{\text{corner}}$, $e^{\text{edge}}_{\text{cont}} \in V^{\text{edge}}$ and $e^{\text{bubble}}_{\text{cont}} \in V^{\text{bubble}}$. The determination of e_{cont} requires to set the proper values for $e^{\text{corner}}_{\text{cont}}$, $e^{\text{edge}}_{\text{cont}}$ and $e^{\text{bubble}}_{\text{cont}}$.

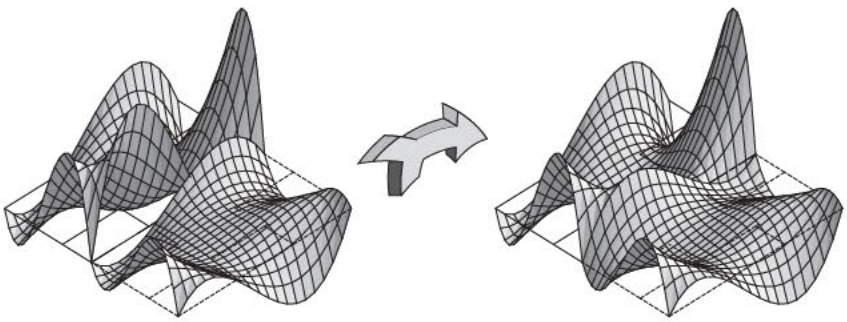

Figure 2. Averaging of the degrees of freedom associated with the edges.

Following Remark 5, e_{cont} is determined starting from e_{est} and such that e_{cont} is likely a good approximation to e_{ref}. The application transforming e_{est} in e_{cont} is denoted by $\mathscr{M}$:

$$\mathscr{M} : V^{\text{ref}}_{\text{brok}} \rightarrow V^{\text{ref}}$$

$$e_{\text{est}} \mapsto e_{\text{cont}}$$

Thus, to characterize the smoothing operator $\mathscr{M}$ it is sufficient to describe e_{cont} as a function of e_{est}, that is $e^{\text{corner}}_{\text{cont}}$, $e^{\text{edge}}_{\text{cont}}$ and $e^{\text{bubble}}_{\text{cont}}$ as functions of $e^{\text{corner}}_{\text{est}}$, $e^{\text{edge}}_{\text{est}}$ and $e^{\text{bubble}}_{\text{est}}$. Indeed, $\mathscr{M}$ is described by the way it maps e_{est} into e_{cont}. Thus, in order to characterize $\mathscr{M}$ it suffices to define the decomposition of the $e_{\text{cont}} = \mathscr{M}(e_{\text{est}})$, that is $e^{\text{corner}}_{\text{cont}}$, $e^{\text{edge}}_{\text{cont}}$ and $e^{\text{bubble}}_{\text{cont}}$, in terms of the original estimate e_{est} or its decomposition.

In order to enforce continuity, the 'corner' and 'edge' components are smoothed independently, that is $e^{\text{corner}}_{\text{cont}} = \mathscr{M}(e^{\text{corner}}_{\text{est}})$ and $e^{\text{edge}}_{\text{cont}} = \mathscr{M}(e^{\text{edge}}_{\text{est}})$. As already mentioned, the simplest option is to average the discontinuous values. In a 2-D framework, every interelement edge Γ_m $(m = 1, \ldots, \text{n}_{\text{int}})$ is shared by two elements, say $\Gamma_m = \overline{\Omega_k} \cap \overline{\Omega_l}$ and, therefore

$$e^{\text{edge}}_{\text{cont}}|_{\Gamma_m} := \tfrac{1}{2}(e^{\text{edge}}_{\text{est}}|_{\Omega_k} + e^{\text{edge}}_{\text{est}}|_{\Omega_l}) \tag{32}$$

see Figure 2 for illustration. The same strategy is adopted for the corner points. The contribution of the interpolation functions associated with the corner points, $e^{\text{corner}}_{\text{cont}}$ is computed averaging the values of the discontinuous function $e^{\text{corner}}_{\text{est}}$ in each corner point. That results in an expression similar to Equation (32) where, for every corner point, the number of values to average is equal to the number of elements to which the corner point belongs. This is illustrated in Figure 3.

Once $e^{\text{corner}}_{\text{cont}}$ and $e^{\text{edge}}_{\text{cont}}$ are set it is necessary to find the value of $e^{\text{bubble}}_{\text{cont}}$. It is worth noting that the choice for $e^{\text{bubble}}_{\text{cont}}$ does not affect the continuity of e_{cont}. The value of $e^{\text{bubble}}_{\text{cont}}$ is therefore selected such that the obtained estimate is as sharp as possible.

Recall that, once e_{cont} is determined, the sharper lower bound is $\varepsilon^{\text{opt}}_{\text{low}}$, see Equation (27). Then, the first idea is to select $e^{\text{bubble}}_{\text{cont}}$ such that, given $e^{\text{corner}}_{\text{cont}}$ and $e^{\text{edge}}_{\text{cont}}$, it maximizes $\varepsilon^{\text{opt}}_{\text{low}}$. However, this criterion leads to a non-linear global (referred to the whole domain) equation which is difficult to solve. On the contrary, finding $e^{\text{bubble}}_{\text{cont}}$ such that $\varepsilon_{\text{low}}(1)$, see Equation (25), is maximum leads to a simple linear local (element by element) equation. This is stated in the following theorem:

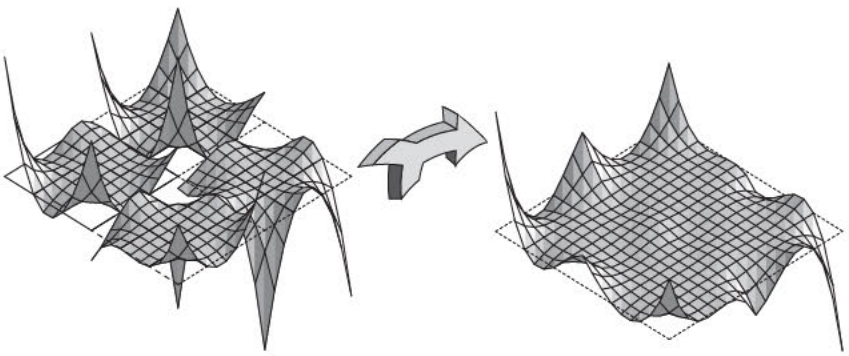

Figure 3. Averaging of the degrees of freedom associated with the corners.

Theorem 3

Let e_{est} be an error estimate verifying the hypothesis of Theorem 1 and, therefore, being an upper bound of the reference error. Let $e_{\text{cont}} = e_{\text{cont}}^{\text{corner}} + e_{\text{cont}}^{\text{edge}} + e_{\text{cont}}^{\text{bubble}}$ be a corrected estimate. Assume that $e_{\text{cont}}^{\text{corner}}$ and $e_{\text{cont}}^{\text{edge}}$ are obtained by averaging. Then, the value of $e_{\text{cont}}^{\text{bubble}}$ maximizing $\varepsilon_{\text{low}}(1)$ is such that

$$a(e_{\text{cont}}^{\text{bubble}}, v) = a(e_{\text{est}} - e_{\text{cont}}^{\text{corner}} - e_{\text{cont}}^{\text{edge}}, v) \quad \forall v \in V^{\text{bubble}} \tag{33}$$

Proof

Recall that $\varepsilon_{\text{low}}(1) = \|e_{\text{est}}\|^2 - \|e_{\text{cont}} - e_{\text{est}}\|^2$, therefore maximize $\varepsilon_{\text{low}}(1)$ is equivalent to minimize

$$\|e_{\text{cont}} - e_{\text{est}}\| = \|e_{\text{cont}}^{\text{bubble}} - (e_{\text{est}} - e_{\text{cont}}^{\text{corner}} - e_{\text{cont}}^{\text{edge}})\|$$

The problem is reformulated as: find $e_{\text{cont}}^{\text{bubble}} \in V^{\text{bubble}}$ such that $\|e_{\text{cont}}^{\text{bubble}} - (e_{\text{est}} - e_{\text{cont}}^{\text{corner}} - e_{\text{cont}}^{\text{edge}})\|$ is minimum. Obviously, the solution of this problem is the projection of $e_{\text{est}} - e_{\text{cont}}^{\text{corner}} - e_{\text{cont}}^{\text{edge}}$ on V^{bubble} which satisfies Equation (33). □

Thus, taking $e_{\text{cont}}^{\text{bubble}}$ as the solution of Equation (33) completes the determination of $\mathcal{M}$. Note that, in this case, e_{cont} depends on the 'corner' and 'edge' components of e_{est}.

Remark 6

The smoothing operator $\mathcal{M}$ is linear because $e_{\text{cont}}^{\text{corner}}$, $e_{\text{cont}}^{\text{edge}}$ and $e_{\text{cont}}^{\text{bubble}}$ are linear functions of $e_{\text{est}}^{\text{corner}}$, $e_{\text{est}}^{\text{edge}}$ and $e_{\text{est}}^{\text{bubble}}$. Moreover, the quality of the lower bound $\varepsilon_{\text{low}}^{\text{opt}}$ depends on the ability of $\mathcal{M}$ to approximate the reference error e_{ref}. Note this quality depends only on the averaging on the boundaries. It suffices that e_{cont} coincides with e_{ref} on the interelement boundaries (i.e. for $e_{\text{cont}}^{\text{corner}} + e_{\text{cont}}^{\text{edge}}$) to obtain an exact error assessment. That is if

$$e_{\text{cont}}|_{\Gamma_m} = e_{\text{ref}}|_{\Gamma_m} \quad \text{for every } m = 1, \ldots, \text{n}_{\text{int}}$$

then $e_{\text{cont}} = e_{\text{ref}}$ and, consequently (see Remark 5),

$$\varepsilon_{\text{low}}^{\text{opt}} = \varepsilon_{\text{low}}(1) = \|e_{\text{ref}}\|^2$$

4.3. Computational aspects

The selection of the optimal value of $e_{\text{cont}}^{\text{bubble}}$ is performed solving Equation (33). These computations can be done locally, element by element, because the bubble spaces are orthogonal (the supports of the bubbles are disjoint). Thus, once $e_{\text{cont}}^{\text{corner}}$ and $e_{\text{cont}}^{\text{edge}}$ are computed by simple averaging, the restriction of $e_{\text{cont}}^{\text{bubble}}$ to Ω_k, $e_{\text{cont}}^{\text{bubble}}|_{\Omega_k}$ is computed solving the local version of Equation (33):

$$a_k(e_{\text{cont}}^{\text{bubble}}|_{\Omega_k}, v) = a_k(e_{\text{est}} - e_{\text{cont}}^{\text{corner}} - e_{\text{cont}}^{\text{edge}}, v) \quad \forall v \in V_k^{\text{bubble}} \tag{34}$$

Equation (34) results in a small system of linear equations that must be solved to compute $e_{\text{cont}}^{\text{bubble}}|_{\Omega_k}$. The number of equations for each local problem is equal to the number of 'bubble' degrees of freedom in the reference discretization. For example, for lagrangian quadrilateral elements, this number is equal to $(1 - \tilde{p})^2$, being $\tilde{p}$ the degree of the polynomials used to generate V^{ref}.

4.4. Assessment of the effectivity index and average estimate

Once the lower bound of the error is computed, the effectivity index of the original estimate $\|e_{\text{est}}\|$ may be easily assessed. Let η_{est} be the effectivity index associated with e_{est},

$$\eta_{\text{est}} := \frac{\|e_{\text{est}}\|}{\|e_{\text{ref}}\|} \tag{35}$$

The upper bound property ensures $\eta_{\text{est}} \geqslant 1$. Nevertheless η_{est} may be very large and it is not possible, in the general case, to assess the quality of the estimate. Using the lower bound ε_{low} of the error, an upper bound of the effectivity index η^+ is easily computed:

$$\eta^+ := \frac{\|e_{\text{est}}\|}{\sqrt{\varepsilon_{\text{low}}}} = \geqslant \eta_{\text{est}} \tag{36}$$

This pessimistic value of the effectivity index is sharp when the lower bound error estimate ε_{low} is sharp.

Once the upper and the lower bounds of the error, $\varepsilon_{\text{upp}} = \|e_{\text{est}}\|^2$ and ε_{low}, are available the average estimate is introduced

$$\varepsilon_{\text{ave}} := \tfrac{1}{2}(\varepsilon_{\text{upp}} + \varepsilon_{\text{low}}) \tag{37}$$

Remark 7

As noted in Remark 2, the estimates $\varepsilon_\star$ represent approximations to the squared norms of the error. The average of the squared norms is larger than the simple averaging of the norms, that is,

$$\tfrac{1}{2}(\varepsilon_{\text{upp}} + \varepsilon_{\text{low}}) \geqslant [\tfrac{1}{2}(\sqrt{\varepsilon_{\text{upp}}} + \sqrt{\varepsilon_{\text{low}}})]^2$$

The behaviour of this average estimate is analysed in the examples presented in Section 6.

5. FITTING LOCAL ARBITRARY CONSTANTS FOR $b = 0$

In problems without a reaction term, the lower bounds of the error obtained with the previously discussed techniques have a poor (very low) eectivity index. In this section, a strategy to

preclude this deficiency is introduced. If $b=0$ in Equation (1) (pure diffusion, no reaction) e_{est} is locally determined up to a constant because

$$\|e_{\text{est}}\|_k = \|e_{\text{est}} + c_k\|_k, \quad k = 1, \ldots, \text{n}_{\text{elem}} \tag{38}$$

Then, the estimate e_{est} may be replaced by $e_{\text{est}} + \sum_{k=1}^{\text{n}_{\text{elem}}} c_k \phi_k$ without changing the upper bound ε_{upp}, being $\{\phi_1, \phi_2, \ldots, \phi_{\text{n}_{\text{elem}}}\}$ the basis of the space of piecewise constant functions. That is, for $k = 1, \ldots, \text{n}_{\text{elem}}$,

$$\phi_k(\mathbf{x}) = \begin{cases} 1 & \text{if } \mathbf{x} \in \Omega_k \\ 0 & \text{if } \mathbf{x} \notin \Omega_k \end{cases} \tag{39}$$

The upper bound estimate ε_{upp} is independent of the constants c_k. Nevertheless, the choice of the constants c_k affects drastically the value of the corrected error, e_{cont}. Moreover, the correction strategy is expected to work properly only if the average values of e_{est} are close to e_{ref}, see Remark 5. If the constants are set arbitrarily, the value of the correction cannot be expected to be optimal.

Consequently, the constants c_k, $k = 1, \ldots, \text{n}_{\text{elem}}$, are taken as unknowns and they are determined such that the resulting lower bound is somehow optimal. Let $\mathbf{c} = [c_1 \ldots c_{\text{n}_{\text{elem}}}]$ be the vector of unknown constants. The corrected estimate e_{cont} may be seen as a function of $\mathbf{c}$:

$$e_{\text{cont}}(\mathbf{c}) := \mathscr{M}\left(e_{\text{est}} + \sum_{k=1}^{\text{n}_{\text{elem}}} c_k \phi_k\right) = \mathscr{M}(e_{\text{est}}) + \sum_{k=1}^{\text{n}_{\text{elem}}} c_k \mathscr{M}(\phi_k) \tag{40}$$

It is clear from Equation (40) that, due to the linearity of $\mathscr{M}$, $e_{\text{cont}}(\mathbf{c})$ is linear. Both the lower bounds $\varepsilon_{\text{low}}(1)$ and $\varepsilon_{\text{low}}^{\text{opt}}$ depend on $\mathbf{c}$ through e_{cont}. The criterion used to select $\mathbf{c}$ is obviously to maximize the lower bound. The maximization of $\varepsilon_{\text{low}}^{\text{opt}}$ is the more natural option because $\varepsilon_{\text{low}}^{\text{opt}}$ is the sharper error bound. Nevertheless, similarly to the previous section, finding $\mathbf{c}$ that optimizes $\varepsilon_{\text{low}}^{\text{opt}}$ requires to solve a non-linear problem. On the contrary, to find $\mathbf{c}$ such that $\varepsilon_{\text{low}}(1)$ is maximum leads to a simple linear problem. Thus, the criterion for determining $\mathbf{c}$ is based on maximizing $\varepsilon_{\text{low}}(1)$ rather than $\varepsilon_{\text{low}}^{\text{opt}}$.

The dependence of $\varepsilon_{\text{low}}(1)$ on $\mathbf{c}$ is written by introducing Equation (40) in Equation (25) and replacing e_{est} by $e_{\text{est}} + \sum_{k=1}^{\text{n}_{\text{elem}}} c_k \phi_k$:

$$\begin{aligned} \varepsilon_{\text{low}}(1) &= \left|\left| e_{\text{est}} + \sum_{k=1}^{\text{n}_{\text{elem}}} c_k \phi_k \right|\right|^2 - \left|\left| e_{\text{est}} + \sum_{k=1}^{\text{n}_{\text{elem}}} c_k \phi_k - \mathscr{M}(e_{\text{est}}) - \sum_{k=1}^{\text{n}_{\text{elem}}} \mathscr{M}(\phi_k) c_k \right|\right|^2 \\ &= \|e_{\text{est}}\|^2 - \left|\left| e_{\text{est}} - \mathscr{M}(e_{\text{est}}) - \sum_{k=1}^{\text{n}_{\text{elem}}} \mathscr{M}(\phi_k) c_k \right|\right|^2 \end{aligned} \tag{41}$$

Then, to maximize $\varepsilon_{\text{low}}(1)$ is equivalent to minimize the function $F(\mathbf{c})$ defined by

$$F(\mathbf{c}) := \left|\left| e_{\text{est}} - \mathscr{M}(e_{\text{est}}) - \sum_{k=1}^{\text{n}_{\text{elem}}} \mathscr{M}(\phi_k) c_k \right|\right|$$

The coefficients c_k that minimize $F(\mathbf{c})$ are obtained imposing that $\sum_{k=1}^{\text{n}_{\text{elem}}} \mathscr{M}(\phi_k) c_k$ is the projection of $e_{\text{est}} - \mathscr{M}(e_{\text{est}})$ on the space generated by the functions $\mathscr{M}(\phi_k)$, for $k = 1 \ldots \text{n}_{\text{elem}}$

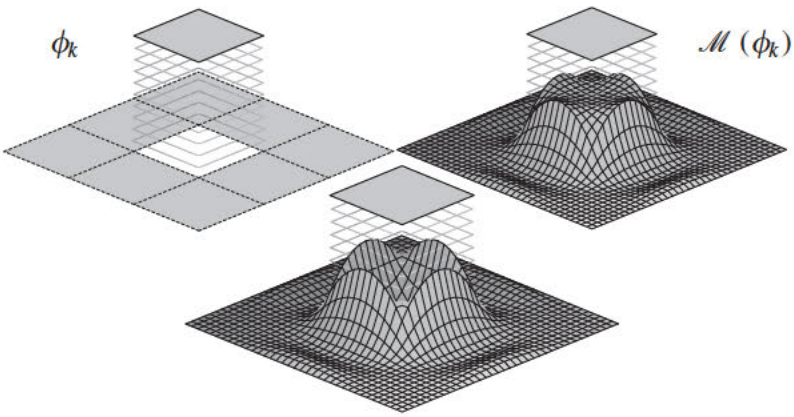

Figure 4. Construction of $\mathcal{M}(\phi_k)$ (right) from ϕ_k (left). The function in the centre accounts only for the 'corner' and 'edge' terms, before adding the 'bubble' term that affects only the interior of the elements. Note that the influence of using the proper 'bubble' contribution is very important.

(that is, the image by $\mathcal{M}$ of the space of piecewise constant functions). Figure 4 illustrates the shape of the functions $\mathcal{M}(\phi_k)$ and their construction from ϕ_k.

Thus, the equation to be satisfied by the coefficients c_k is

$$\sum_{k=1}^{n_{elem}} c_k a(\mathcal{M}(\phi_k), \mathcal{M}(\phi_l)) = a(e_{est} - \mathcal{M}(e_{est}), \mathcal{M}(\phi_l)) \quad \text{for } l = 1, \ldots, n_{elem} \tag{42}$$

That is, $\mathbf{c}$ is computed as the solution of a linear $n_{elem} \times n_{elem}$ system of equations.

Once the coefficients c_k are computed, the corresponding corrected estimate e_{cont} is introduced in the expression of ε_{low}^{opt} to obtain the sharper error lower bound.

Numerical experiments demonstrate that the correction obtained with this strategy yields sharp lower bound estimates because the obtained correction e_{cont} is a much better approximation to e_{ref}, see Figure 5. On the contrary, the correction for the standard estimate (i.e. with arbitrary constants) yields lower bound estimates of poor quality.

It is worth noting that the constants c_k are determined solving the global system of equations (42). Thus, adding these constants to the original estimate e_{est} accounts for the influence of the whole domain in the local errors. Consequently, the estimate e_{cont} using this information may be used to assess the pollution errors, that is, the errors affecting each zone of the domain coming from far from its close neighbourhood.

6. NUMERICAL EXAMPLES

We study in this section the behaviour of the postprocessing estimate presented above. The examples selected are such that the analytical exact solution is known and they have been used by other authors to assess the performance of similar techniques [1, 2]. The quality of the error estimates is measured using the index ρ

$$\rho = \frac{\text{estimated error}}{\text{exact (or reference) error}} - 1$$

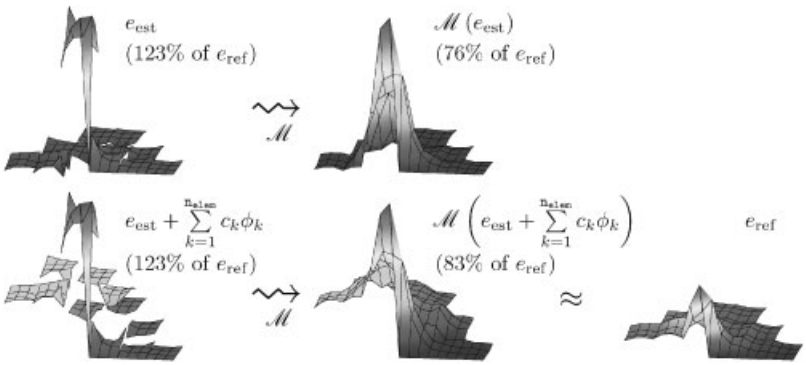

Figure 5. Illustration of the constant fitting process: the raw estimate e_{est} with arbitrary constants is smoothed into $\mathscr{M}(e_{\text{est}})$ (top), the smoothed version of the estimate corrected with the optimal constants is much more similar to the reference error (bottom): in the example the underestimation is improved from 76% (without constant fitting) to 83%.

that is, the effectivity index minus one. The use of ρ is preferred because the sign of ρ indicates if the estimate is an upper or a lower bound (positive if upper, negative if lower) and the absolute value indicates the quality of the estimate (good quality if $|\rho|$ small). In the following, the value of ρ corresponding to every estimate is denoted with the same subscript, that is,

$$\rho_{\star} = \frac{\sqrt{\varepsilon_{\star}}}{\|e\|} - 1$$

where the subscript ★ takes the values 'upp', 'low' and 'ave'. The superscript C for ρ_{low}, $\rho^{\text{C}}_{\text{low}}$, is used to denote the correction obtained with the determination of elementwise constants introduced in Section 5. Moreover, we also use the version ρ^{+} corresponding to the assessed effectivity index η^{+} ($\rho^{+} := \eta^{+} - 1$), see Equation (36).

As noted in Section 3.4, the second and third estimators introduced in Reference [1], denoted by e_2 and e_3, respectively, are used as the original upper bound estimates e_{est}. In the examples, the performance of these estimates is analysed throughout the values of ρ_{upp}.

6.1. Example 1

In the first example the reaction–diffusion equation is solved, $a = 1$ and $b = 1$ in Equation (1). The problem is defined in the squared domain $\Omega = (0,1)\times(0,1)$. The boundary conditions are set to be Dirichlet homogeneous (that is $u = 0$) on $\Gamma_D := \{(x,0); 0 \leqslant x \leqslant 1\}$ and Neumann homogeneous (that is $\partial u/\partial n = 0$) elsewhere on $\partial\Omega$. The source term s is taken such that the exact solution has the following analytical expression:

$$u(x,y) = \frac{1}{2000}\, x^2(1-x)^2 \mathrm{e}^{10x^2} y^2(1-y)^2 \mathrm{e}^{10y} \tag{43}$$

see Figure 6 for a representation. The second example described in this section is stated such that the solution u is exactly the same.

The approximate solution u_h is computed using a bilinear interpolation ($p = 1$) whereas the error estimates e_2 and e_3 are computed using a bicubic interpolation ($\tilde{p} = 3$).

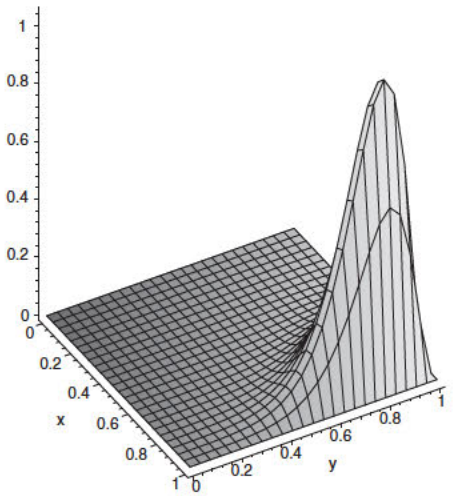

Figure 6. Examples 1 and 2: exact solution.

Table I. Example 1: results in a series of uniformly h-refined meshes.

			Estimate e_2				Estimate e_3			
Dof	$\|\|e\|\|/\|\|u\|\|$	$\|\|e_{\text{ref}}\|\|/\|\|u\|\|$	ρ^+	ρ_{upp}	ρ_{low}	ρ_{ave}	ρ^+	ρ_{upp}	ρ_{low}	ρ_{ave}
36	0.8469	0.7726	0.3453	0.1589	−0.1386	0.0210	0.2713	0.0544	−0.1706	−0.0514
121	0.4331	0.4036	0.2428	0.1221	−0.0971	0.0184	0.2116	0.0569	−0.1277	−0.0310
441	0.3083	0.3064	0.3258	0.2132	−0.0849	0.0745	0.2737	0.1706	−0.0809	0.0524
1681	0.2093	0.2092	0.2578	0.1831	−0.0594	0.0688	0.1843	0.1263	−0.0489	0.0424
6561	0.1144	0.1144	0.1129	0.0845	−0.0255	0.0310	0.0691	0.0498	−0.0181	0.0164

The proposed approach is used to recover new estimates in two sequences of increasingly refined meshes. In the first series of meshes the refinement is uniform, in the second one the refinement follows an adaptive strategy based on the error assessment [14].

The results concerning the uniformly refined meshes are summarized in Table I and Figure 7.

In a similar manner, the results concerning the adaptively refined meshes are summarized in Table II and Figure 8. The sequence of adapted meshes is shown in Figure 9.

It is worth noting in Tables I and II that the difference between the exact error (in this case is known) and the reference error is negligible for accurate enough meshes. As expected, the values of ρ_{upp} are indeed positive and the values of ρ_{low} negative. The value of ρ^+ is greater than ρ_{upp}. Note that ρ^+ is computed without any information on the exact (or reference) solution but it furnishes a good approximation of the exact effectivity index. Moreover, for most of the meshes (except for the coarsest) the value of the corrected estimate ε_{low} is better than the original estimate ε_{upp} ($|\rho_{\text{low}}| < |\rho_{\text{upp}}|$), that results on $\rho_{\text{ave}} > 0$.

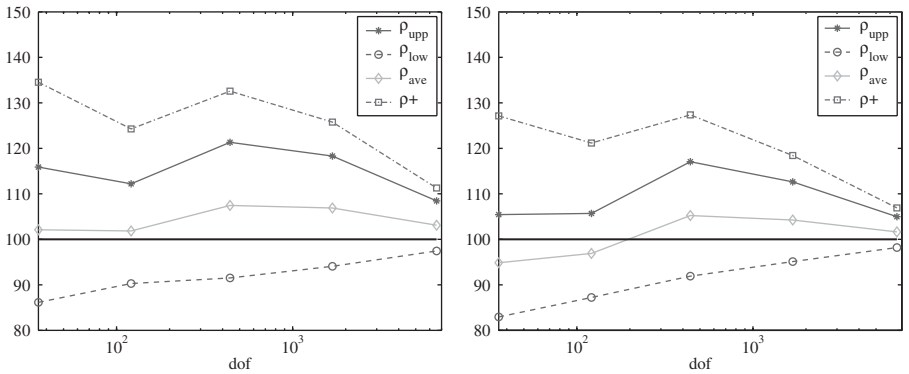

Figure 7. Example 1: performance of the estimates following a uniform *h*-refinement process for the estimates e_2 (left) and e_3 (right).

Table II. Example 1: results in a series of adaptively *h*-refined meshes.

			Estimate e_2				Estimate e_3			
Dof	$\|\|e\|\|/\|\|u\|\|$	$\|\|e_{ref}\|\|/\|\|u\|\|$	ρ^+	ρ_{upp}	ρ_{low}	ρ_{ave}	ρ^+	ρ_{upp}	ρ_{low}	ρ_{ave}
36	0.8469	0.7726	0.3453	0.1589	−0.1386	0.0210	0.2713	0.0544	−0.1706	−0.0514
2550	0.0798	0.0798	0.0822	0.0645	−0.0164	0.0248	0.0517	0.0354	−0.0155	0.0103
2905	0.0478	0.0478	0.1263	0.1136	−0.0113	0.0530	0.1129	0.0622	−0.0456	0.0098
3574	0.0433	0.0433	0.1279	0.1152	−0.0113	0.0539	0.1108	0.0614	−0.0445	0.0098

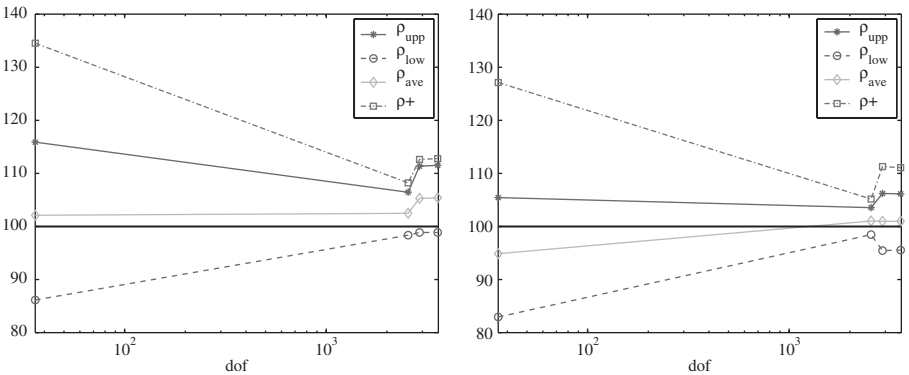

Figure 8. Example 1: performance of the estimates following an adaptive *h*-refinement process for the estimates e_2 (left) and e_3 (right)

Remark 8

As expected, the adaptive procedure optimizes the computational resources and yields lower error with less degrees of freedom. However, the adapted meshes have distorted elements, see Figure 9, and the quality of the estimates e_2 and e_3 is slightly degraded in adapted meshes, see Figure 8. This phenomenon produces a peculiar end effect in the plots describing the evolution of the effectivity along the adaptive process. This effect does not appear in the

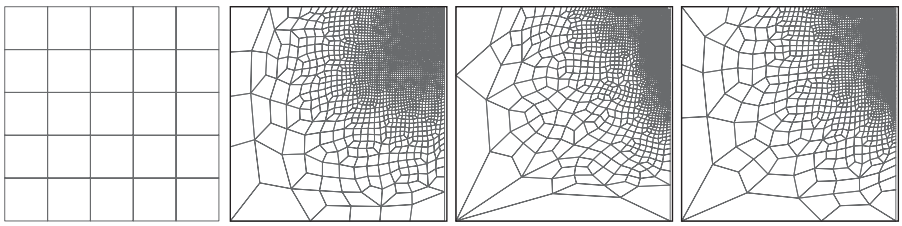

Figure 9. Example 1: Sequence of adapted meshes with $36, 2550, 2950$ and 3574 dof.

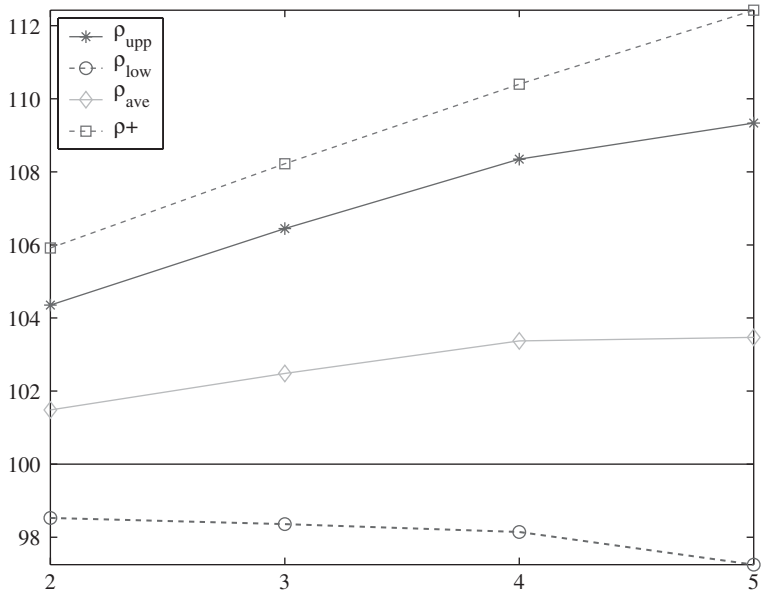

Figure 10. Example 1: performance of the estimators and using different degrees of interpolation in the reference space ($\tilde{p}$).

uniform h-refinement process where all the meshes are structured, see Figure 7. The proposed lower bound corrects this behaviour in the case of the estimate e_2 but not in the case of e_3. In this example, the average ε_{ave} performs very well in the sense that behaves as a new estimate, mostly a new upper bound, much more reliable than the original one. The same effect is observed in the next example, see Figure 11.

The effect of varying the degree of interpolation in the reference space ($\tilde{p}$) is investigated for one of the meshes (the second mesh of the adaptive process, with 2550 dof) and for the estimate e_2. We are interested in assessing the influence of $\tilde{p}$ in the error estimate and the corresponding corrections. The results are shown in Figure 10. Note that the effectivity of the original estimate, e_{est} is not improved by using a larger $\tilde{p}$. On the contrary, the larger values of $\tilde{p}$ are associated with the poorer quality estimates. Nevertheless, the quality of the postprocessed lower bounds is not so sensitive to the variations of $\tilde{p}$ and their quality does not depend on $\tilde{p}$.

Table III. Example 2: results in a series of uniformly h-refined meshes.

			Estimate e_2				
Dof	$\|\|e\|\|/\|\|u\|\|$	$\|\|e_{\text{ref}}\|\|/\|\|u\|\|$	ρ^+	ρ_{upp}	ρ_{low}	$\rho^{\text{C}}_{\text{low}}$	ρ_{ave}
36	0.8483	0.7737	0.2729	0.1571	−0.1177	−0.0909	0.0405
121	0.4342	0.4046	0.2059	0.1217	−0.0838	−0.0698	0.0304
441	0.3091	0.3072	0.2220	0.2131	−0.0461	−0.0073	0.1084
1681	0.2099	0.2098	0.1844	0.1831	−0.0321	−0.0011	0.0949
6561	0.1148	0.1148	0.0849	0.0845	−0.0148	−0.0003	0.0430

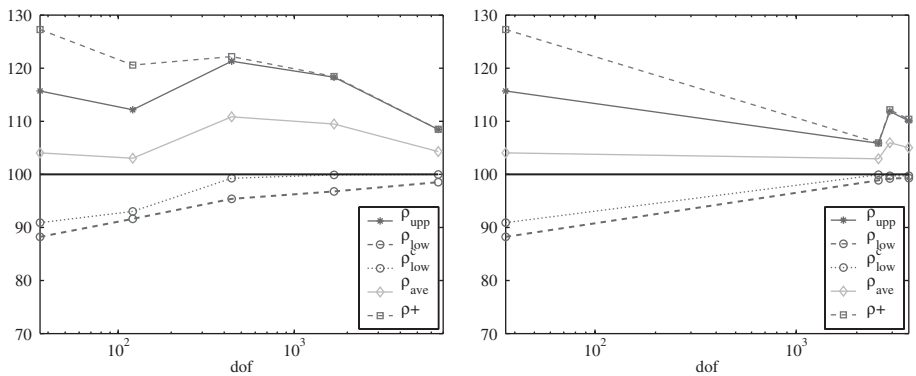

Figure 11. Example 2: performance of the estimates following a uniform (left) and an adaptive (right) h-refinement process for the estimate e_2.

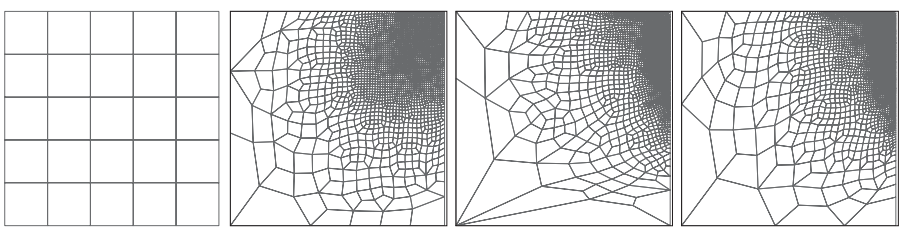

Figure 12. Example 2: sequence of adapted meshes with 36, 2561, 2918 and 3628 dof.

6.2. *Example 2*

Now, we consider the Poisson equation, $a = 1$ and $b = 0$ in Equation (1). The domain and the boundary conditions are exactly the same as in the previous example. The source term s is taken such that the exact solution is also the same, see Equation (43). In this example, we only study the application of the developed postprocessing strategy to the e_2 estimate.

Again, the proposed strategy is used in a series of uniformly and adaptively h-refined meshes. The results for the uniformly refined meshes are summarized in Table III and Figure 11. Figure 12 shows a sequence of adapted meshes and Table IV with Figure 11 describe the behaviour of the different estimates. The notation $\rho^{\text{C}}_{\text{low}}$ is introduced to denote the

Table IV. Example 2: results in a series of adaptively h-refined meshes.

			Estimate e_2				
Dof	$\|\|e\|\|/\|\|u\|\|$	$\|\|e_{\text{ref}}\|\|/\|\|u\|\|$	ρ^+	ρ_{upp}	ρ_{low}	$\rho_{\text{low}}^{\text{C}}$	ρ_{ave}
36	0.8483	0.7737	0.2729	0.1571	−0.1177	−0.0909	0.0405
2561	0.0785	0.0785	0.0593	0.0586	−0.0112	−0.0007	0.0294
2918	0.0482	0.0482	0.1216	0.1186	−0.0077	−0.0027	0.0596
3628	0.0432	0.0432	0.1038	0.1008	−0.0070	−0.0027	0.0503

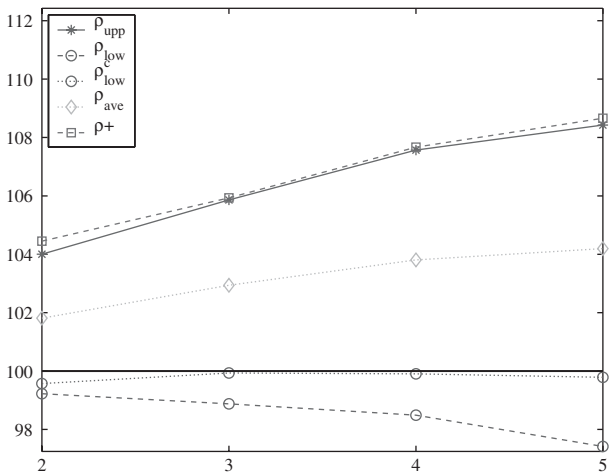

Figure 13. Example 2: performance of the estimators and using different degrees of interpolation in the reference space ($\tilde{p}$).

correction introduced in Section 5. As expected, the value of $\rho_{\text{low}}^{\text{C}}$ is much better than the value of ρ_{low}.

The influence of $\tilde{p}$ in the different estimates is shown in Figure 13. These results correspond to the second mesh of the adaptive process, with 2561 dof. Once again, due to the phenomenon described in the previous example, increasing $\tilde{p}$ does not result in a better effectivity index for the upper bound estimate. Nevertheless, the lower bound estimate e_{cont} with the constant element by element correction (measured by $\rho_{\text{low}}^{\text{C}}$) is roughly independent of $\tilde{p}$ and much better compared to the original estimate.

6.3. *Example 3*

This example was introduced in Reference [1]. We consider the Laplace equation, $a=1$, $b=0$ and $s=0$ in Equation (1). As in the previous example, only the e_2 estimate is used with the proposed postprocessing strategy.

The domain Ω is defined by $\Omega=\{(r,\theta) : 0<r<1,\ 0<\theta<k\pi/4\}$ where r and θ are the polar coordinates and the analytical solution is

$$u(r,\theta)=r^{2/k}\sin\left(\frac{2\theta}{k}\right) \tag{44}$$

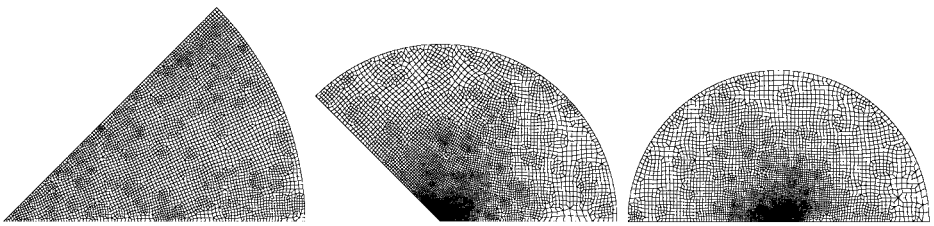

Figure 14. Example 3: adapted meshes for $k=1$ (left) $k=3$ (centre) and $k=4$ (right).

Table V. Example 3, $k=1$: results in a series of adaptively h-refined meshes.

			Estimate e_2				
Dof	$\|\|e\|\|/\|\|u\|\|$	$\|\|e_{\text{ref}}\|\|/\|\|u\|\|$	ρ^+	ρ_{upp}	ρ_{low}	$\rho_{\text{low}}^{\text{C}}$	ρ_{ave}
69	0.0397	0.0397	0.3788	0.3730	−0.0109	−0.0042	0.1993
1637	0.0069	0.0069	0.1250	0.1224	−0.0052	−0.0022	0.0619
3938	0.0044	0.0044	0.1925	0.1849	−0.0109	−0.0064	0.0934
4668	0.0040	0.0040	0.2051	0.1992	−0.0092	−0.0048	0.1019

Table VI. Example 3, $k=3$: results in a series of adaptively h-refined meshes.

			Estimate e_2				
Dof	$\|\|e\|\|/\|\|u\|\|$	$\|\|e_{\text{ref}}\|\|/\|\|u\|\|$	ρ^+	ρ_{upp}	ρ_{low}	$\rho_{\text{low}}^{\text{C}}$	ρ_{ave}
169	0.0298	0.0294	1.0167	0.6153	−0.2412	−0.1991	0.2749
580	0.0139	0.0138	0.7023	0.3618	−0.2468	−0.2001	0.1168
1436	0.0078	0.0077	0.4700	0.3375	−0.1211	−0.0901	0.1438
3795	0.0047	0.0047	0.3860	0.3242	−0.0626	−0.0446	0.1546
6585	0.0036	0.0035	0.3407	0.2861	−0.0615	−0.0407	0.1345

That is, Ω is a circular sector and k is a parameter that sets both the size of the domain and the regularity of the solution. In the following, we consider the cases $k=1,\ 3$ and 4. Dirichlet boundary conditions are imposed along $\theta=0$ and Neumann boundary conditions are forced on the rest of the boundary. The boundary conditions are such that the exact solution is the analytical expression given in Equation (44).

For each one of the values of k, the error assessment is performed for a sequence of adapted meshes. Figure 14 shows examples of adapted meshes for each value of k.

The results are shown in Tables V, VI and VII for $k=1,3$ and 4, respectively, and also in Figure 15. It is worth noting that using the constant fitting (the difference between $\rho_{\text{low}}^{\text{C}}$ and ρ_{low}, see Figure 15) is relevant specially for $k=4$, that is, when the singularity pollutes the error estimate based only on local computations.

In order to analyse the spatial distribution of the estimated error, Figure 16 shows the histograms describing the occurrences of the values of local (element by element) effectivity indices for both the estimated error and the lower estimate. The example corresponds to the second mesh obtained for $k=1$ (with 1637 dof). An almost uniform distribution is obtained

Table VII. Example 3, $k=4$: results in a series of adaptively h-refined meshes.

			Estimate e_2				
Dof	$\|e\|/\|u\|$	$\|e_{\text{ref}}\|/\|u\|$	ρ^+	ρ_{upp}	ρ_{low}	$\rho^{\text{C}}_{\text{low}}$	ρ_{ave}
220	0.1310	0.1200	0.4449	0.1384	−0.2960	−0.2121	−0.0211
372	0.0587	0.0548	0.4858	0.2090	−0.2626	−0.1863	0.0304
723	0.0312	0.0297	0.5364	0.2418	−0.2603	−0.1917	0.0477
3297	0.0126	0.0122	0.4800	0.2293	−0.2346	−0.1694	0.0491
6859	0.0077	0.0076	0.4154	0.2440	−0.1790	−0.1211	0.0770

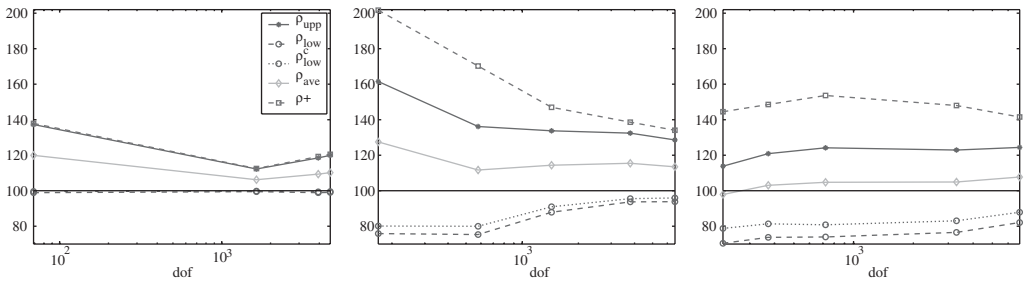

Figure 15. Example 3: performance of the estimates following an adaptive h-refinement for $k=1$ (left), $k=3$ (centre) and $k=4$ (right).

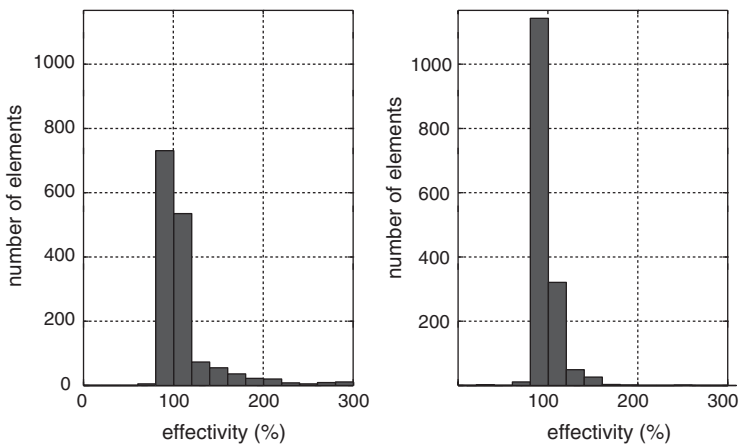

Figure 16. Example 3: Histogram representing the occurrences of the local effectivity index for e_2 (left) and for the proposed strategy (right).

since the values are close to 100%. As expected, the second Bank and Weiser estimator e_2 produces local estimates which overestimate almost everywhere the exact error. The local corrected estimates, as expected, underestimate the exact error. The bound property for the global error is then reproduced locally in most elements.

7. CONCLUDING REMARKS

A simple postprocessing strategy has been presented to recover lower bound estimates from standard residual estimators producing upper bounds of the error. The main idea is to smooth the discontinuous estimate e_{est} and to obtain a continuous approximation e_{cont} to the reference error e_{ref}. A lower bound of the error is computed using e_{cont}.

For the pure diffusion problem (when the reaction term in the PDE vanishes) the estimate e_{est} is determined up to a local (element by element) constant. In order to improve the postprocessing in this situation the local arbitrary constants are found such that the sharpest lower bound is obtained.

Numerical experiments show that the proposed strategy furnishes sharp lower estimates, of better quality than the original upper ones.

The presented strategy may be used in the framework of error estimation for outputs of interest, where upper and lower bounds of the energy error measure are required.

REFERENCES

1. Bank RE, Weiser A. Some a posteriori error estimators for elliptic partial differential equations. *Mathematics of Computation* 1985; **44**:283–301.
2. Ainsworth M, Oden JT. A unified approach to a posteriori error estimation using element residual methods. *Numerische Mathematik* 1993; **65**:25–30.
3. Ladevèze P, Leguillon D. Error estimation procedures in the finite element method and applications. *SIAM Journal on Numerical Analysis* 1983; **20**:485–509.
4. Ladevèze P, Pelle JP, Rougeot PH. Error estimation and mesh optimization for classical finite elements. *Engineering Computations* 1991; **8**:69–80.
5. Díez P, Egozcue JJ, Huerta A. A posteriori error estimation for standard finite element analysis. *Computer Methods in Applied Mechanics and Engineering* 1998; **163**:141–157.
6. Huerta A, Díez P. Error estimation including pollution assessment for nonlinear finite element analysis. *Computer Methods in Applied Mechanics and Engineering* 2000; **181**:21–41.
7. Oden JT, Prudhomme S, Westermann TA, Bass JM. Progress on practical methods of error estimation for engineering calculations. In *Proceedings of the 2nd European Conference on Computational Mechanics*, ECCOMAS & IACM, Cracow, 2001.
8. Paraschivoiu M, Peraire J, Patera A. A posteriori finite element bounds for linear-functional outputs of elliptic partial differential equations. *Computer Methods in Applied Mechanics and Engineering* 1997; **150**:289–312.
9. Ainsworth M, Oden JT. *A Posteriori Error Estimation in Finite Element Analysis* (1st edn). Wiley: Chichester, 2000.
10. Babuška I, Strouboulis T, Gangaraj SK. Guaranteed computable bounds for the exact error in the finite element solution. Part I: One dimensional problem. *Computer Methods in Applied Mechanics and Engineering* 1999; **176**:51–79.
11. Strouboulis T, Babuška I, Gangaraj SK. Guaranteed computable bounds for the exact error in the finite element solution. Part II: bounds for the energy norm of the error in two dimensions. *International Journal for Numerical Methods in Engineering* 2000; **47**:427–475.
12. Prudhomme S, Oden JT. Simple techniques to improve the reliability of a posteriori error estimates for finite element approximations. In *Proceedings of the 2nd European Conference on Computational Mechanics*, ECCOMAS & IACM, Cracow, 2001.
13. Díez P, Parés N, Huerta A. Simple assessment of the effectivity index of residual a posteriori error estimators: recovering lower bounds. In *Proceedings of the 2nd European Conference on Computational Mechanics*, ECCOMAS & IACM, Cracow, 2001.
14. Díez P, Huerta A. A unified approach to remeshing strategies for finite element *h*-adaptivity. *Computer Methods in Applied Mechanics and Engineering* 1999; **176**:215–229.
15. Díez P, Parés N, Huerta A. Obtention de bornes supérieures et inférieures de l'erreur avec des estimateurs résiduels. In *Proceedings of the 5th* '*Colloque National en Calcul des Structures*' CSMA, Giens, 2001.